Ghost imaging: Open secrets and puzzles for undergraduates

Lorenzo Basano[a)] and Pasquale Ottonello
Dipartimento di Fisica, Università di Genova, Via Dodecaneso 33, 16146 Italy

(Received 8 June 2006; accepted 5 January 2007)

Ghost imaging, a novel technique in which the object and the image system are on separate optical paths, was first demonstrated using entangled photon pairs. This demonstration caused it to be regarded as a purely quantum effect, but subsequent work gave wide support to a classical explanation. We provide an introduction to ghost imaging based more on intuition than on formalism and discuss several experiments that can be implemented in a university physics laboratory. © *2007 American Association of Physics Teachers.*
[DOI: 10.1119/1.2437745]

I. INTRODUCTION

The history of ghost imaging began shortly after the birth of ghost interference. Although we will consider only the former technique, our discussion will be clearer if we begin with the latter. In 1995 Klyshko and co-workers published an intriguing paper on two-photon ghost interference and diffraction.[1] A pair of entangled photons (conventionally called the *signal* and the *idler*) are produced by spontaneous parametric down conversion[2,3] and sent along two different paths. A double slit is placed only in the signal arm, and the two photons of each pair are eventually revealed by two distant pointlike detectors. As expected, no first order interference pattern can be detected behind the double slit, due to the insufficient spatial coherence of the individual beams. Nevertheless, an interference pattern can be observed by counting coincidences between the fixed detector and the idler detector as the latter is moved in a transverse direction. The amazing aspect of this result is that the interference pattern is revealed by moving the detector in the path that does not contain the double slit (hence the name *ghost*). Because the explanation of this surprising result is related to the nonlocal correlations of entangled photons, the experiment was classified as a purely quantum effect belonging to the EPR (Einstein-Podolsky-Rosen) type.

In ghost imaging[4] the apparatus differs slightly from the interference setup we just described. A double slit is placed in the signal arm, but now the purpose of the experiment is to retrieve a ghost image of the double slit rather than the interference pattern produced by it. To achieve this goal, all photons passing through the double slit are conveyed onto a "bucket" detector located in the focal plane of a collecting lens. The bucket detector can only reveal photon arrivals and cannot gain any information on the aperture shape. The detector placed in the other arm (the idler) cannot acquire any information about the aperture because photons arriving at it followed the path where the double slit was absent. It is remarkable that an image of the double slit can be retrieved by correlating the outputs of two detectors, neither of which conveys information about the shape of the aperture. In this case, too, the use of the term "ghost" is appropriate.

More recently the results of these experiments on ghost interference and ghost imaging were described as purely nonlocal quantum effects, not amenable to a classical interpretation.[4,5]

Bennink *et al.*[6] have realized a conceptually remarkable experiment that satisfied the protocol of ghost imaging and was based on a classical source of light. Their apparatus creates a pair of very thin rays whose propagation directions are individually random but spatially correlated and thus mimic the spatial behavior of an entangled photon pair.[7] Their experiment is able to emulate the imaging capability of the spontaneous parametric down conversion apparatus because the latter exploits only the spatial correlation of the beams (while correlations linking other properties of entangled photons such as phase, energy, and polarization are not used). Later, Lugiato and co-workers showed that classical ghost imaging can be produced not only by needlelike beams but also by speckle beams of extended cross section.[8–10] This result confirmed that the essential nature of ghost imaging is in the mutual spatial correlation of the beams, whose nature might be quantum (entangled photon pairs) or classical (correlated needlelike rays or pairs of beams endowed with random internal speckles). In either case a ghost image can be retrieved using a suitable data processing technique.

We begin our introduction to ghost imaging by discussing the needlelike beam pair because it lets us use elementary classical reasoning without losing sight of the essential elements of ghost imaging. Although our description is initially simple, it later involves more complex ideas such as the statistical features of speckle patterns and the basic elements of convolution. We have tried to meet the needs of a wide readership by describing the main mathematical tools that will enable as many readers as possible to follow our presentation.

The paper is organized as follows. In Sec. II we describe how a ghost image arises from the use of the apparatus in Ref. 6. The discussion of this experiment is very informative because it emphasizes the fundamental role played in ghost imaging by the mutual spatial correlation of the beams. In Sec. III we follow Refs. 8–10 and ask if needlelike rays are really necessary and what the consequences are of using beam pairs of extended and internally structured cross section, such as those produced by quasi-thermal light sources.[11] We will see that two main cases, which require distinct treatments, should be considered according to whether the average speckle size is comparable to the details of the object to be imaged (Sec. III A) or much smaller (Sec. III B). At this point, we will have described the relevant classical procedures for obtaining ghost imaging, but we will still lack an interpretation of the original ghost imaging experiments based on entangled photon pairs. This gap is filled in Sec. IV. Appendix A is a brief primer on the main statistical features of speckle patterns, and Appendix B offers a detailed de-

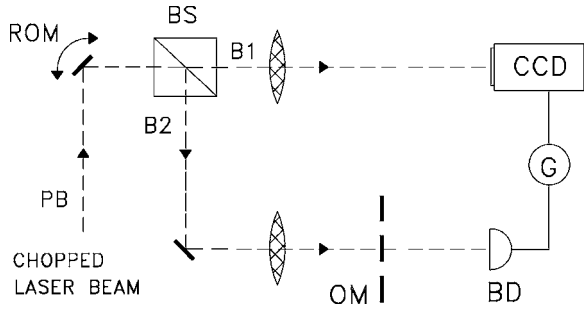

Fig. 1. Schematic of the experimental setup used with a needlelike source. PB: primary beam; ROM: randomly oscillating mirror; BS: 50% beam splitter; B1: image beam; CCD: camera; B2: object beam; OM: object mask; BD: bucket detector for measuring the total intensity going through the mask; and G: gate allowing the camera to record the images.

scription of the experimental apparatus. Appendix C explains the much debated case of ghost imaging produced by quasithermal light.

II. AN ELEMENTARY IMPLEMENTATION OF GHOST IMAGING (RANDOMLY DEFLECTED NEEDLELIKE CLASSICAL BEAMS)

As mentioned in Sec. I, the apparatus described in Ref. 6 created a true ghost image of a mask and required only a classical description. Ghost imaging was described as "a novel imaging method in which the object and imaging system are on different optical paths and are illuminated separately by correlated optical fields."[6]

Figure 1 illustrates the setup used in Ref. 6. In the following we do not use the terms "idler" and "signal," which are used for quantum entangled photons, and refer to the two beams as "image" and "object." The chopped primary beam (PB) is first randomly deflected about the forward direction by the randomly oscillating mirror (ROM) and is then divided by the beam splitter BS into two identical beams B1 and B2. The image beam B1 is sent to the CCD camera. The object beam B2 is passed through the transparent mask OM (the object to be reconstructed). Suppose that OM consists of an opaque mask pierced by three circular holes of equal sizes, H1, H2, and H3 (see Fig. 2). The total intensity of B2 exiting the mask is measured by the bucket detector BD, which is activated by the arrival of photons that have crossed the mask's openings. The activation of BD does not depend on which hole the photons have gone through (photons revealed by the bucket detector convey no information about the shape of the mask). The gate G provides an enable signal to the CCD camera, depending on the value of the bucket detector output. In this experiment the travel directions of beams B1 and B2 are individually random but strongly correlated. If, at a certain instant, we know where one beam is going, we can tell exactly where the other one is heading.

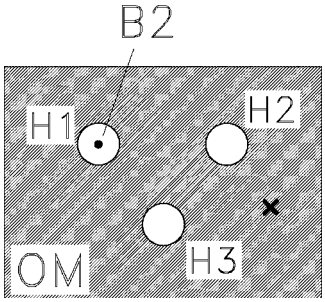

Fig. 2. Object mask consisting of three holes of equal size pierced in an opaque material. The symbols • and × exemplify two points at which the beam B2 may hit the mask. In our experiment the hole diameter is 1 mm and the hole-to-hole distance is 4 mm.

Let's now see how a faithful copy of the mask can be obtained and why it can be called a ghost image. By the proper control of the mirror oscillations, the object ray B2 can be made to hit the mask OM at some random position with almost uniform probability. This position may lie either within one of the holes or in the opaque part of the mask. For example, consider the two cases shown in Fig. 2. In the first, the object ray B2 goes right through the center of H1, and then proceeds past the mask until it reaches the bucket detector which, in turn, enables the CCD camera to record the event. Because of the strict angular correlation of the two rays, image ray B1 will hit the CCD camera (and be recorded by it) at a position that corresponds to the center of H1. For the case that B2 does not meet a hole, the ray is absorbed by the opaque portion of the mask, and no gate pulse is delivered to the CCD camera and no event is recorded. Thus, as the images are acquired and summed in the video board memory, a clear image of the three holes will emerge after a large number of trials. Note that there is no quantum element in this process, nor are photons necessary to implement it. For example, bullet pairs fired against a metal mask by properly correlated guns would produce an equivalent effect. In this setup all the CCD images are formed only by photons that travel in the arm where there is no mask, and hence the apparatus satisfies the definition of ghost imaging given in Ref. 6.

In the simplest form described here, a ghost-image apparatus can be interpreted as the optical version of the key duplicator at a hardware store. A faithful copy of a key is obtained because the position of the milling head (in our case ray B1) is strongly correlated with the position of the tip sensing the object profile (in our case ray B2). Nobody would maintain that the key duplicator is a nonclassical device because the milling head does not interact locally with the original object. It is the spatial correlation between the sensing tip and the milling head that allows us to create a faithful copy of the original key.

The logic of the needlelike rays experiment performed in Ref. 6 is strikingly similar to that of the quantum experiment, which employed entangled photons.[4] More general questions naturally arise. For example, to what extent can the true nature of ghost imaging be regarded as a quantum effect?

III. GHOST IMAGING WITH THERMAL LIGHT: PRELIMINARY COMMENTS

In this section some knowledge of speckles and their main statistical features[12] is required. Appendix A describes the physical origin of speckles and their relevant properties.

The idea that the crucial element in ghost imaging is the spatial correlation of two beams received an important confirmation in Refs. 8–10 in which it was shown that ghost imaging can also be obtained classically when the cross-sectional area of each beam is not negligible and exhibits random intensity fluctuations that render the illumination of the mask completely incoherent. Even though no first order interference effect is detectable behind the object, the corre-

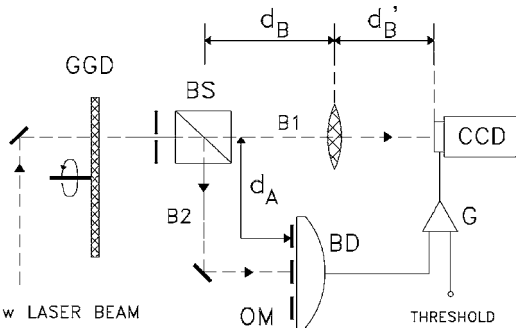

Fig. 3. Same setup as in Fig. 1, with the needlelike source replaced by quasi-thermal light. A threshold control has been added in the object channel to improve the visibility of the final image.

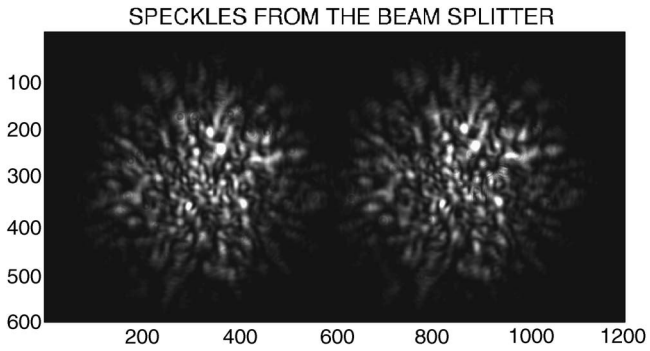

Fig. 4. Sample of a twin speckle pair: one impinges on the CCD camera, the other one on the object mask.

lation of the two beams lets a faithful image of the aperture emerge by properly designed processing, as explained in the following.

At first sight, the goal of obtaining a ghost image using extended incoherent beams might seem hopeless. Recall that the success of the experiment in Ref. 6 relies on the fact that the beam pairs in their apparatus are pointlike and correlated. So even though the CCD camera does not receive photons that went through the mask, it records the position of their twins that are translated with respect to the former by a fixed amount (which is also the secret of ghost imaging produced by entangled photon pairs). This explanation of ghost imaging is simple as the key duplicator analogy reveals. If the needlelike rays of Sec. II are replaced by beams of nonzero cross section, each beam's cross section exhibits a random intensity structure (speckles), and the beam cross sections are larger than the object to be copied. In this case the point reconstruction of the image that is justified in Ref. 6 can no longer be invoked.

We emphasize the essential change that takes place when we shift from needlelike rays to extended speckle beams. With needlelike rays, each frame contributes to the final image with a single bright dot whose position is inside an area that corresponds geometrically to one of the holes. Bright dots falling outside the three hole areas cannot activate the camera gate (see Fig. 2). Ideally, the camera accumulates bright dots according to a noiseless reconstruction, that is, there will be light inside the hole images and dark outside them.

With speckle beams, each frame grabbed by the CCD camera is a random collection of bright and dark patches (speckles) covering an area larger than the mask. In each frame there may be light where the mask image necessitates dark, which implies the occurrence of a large amount of noise; it is difficult to visualize how the sum of such random and noisy images will be able to reproduce the ordered pattern of the mask. An explanation of this successful reproduction requires subtle statistical considerations that we will now describe.

In Fig. 3 beams B1 and B2 create (on any plane they intersect) two random speckle patterns whose average granularity is much smaller than the beam cross section; each of the beams is then spatially incoherent. Because B1 and B2 are generated from a single beam that divides at a 50%–50% beam splitter, they are mutually coherent and generate a pair of identical speckle patterns in the object and in the image planes (see Fig. 4). This description can explain many results of ghost imaging that were often ascribed to quantum behavior. But quantum mechanics is not needed, nor is it needed to explain the famous Hanbury-Brown and Twiss spatial correlations.[13] The goal of ghost imaging with random light is to reconstruct an image of the mask under the following conditions:

(1) The instantaneous speckle pattern falling on the CCD camera is produced by B1, that is, by the beam that never interacts with the object. If we would simply sum all the speckle patterns falling on the CCD camera, we would not obtain anything but noise.
(2) The instantaneous speckle pattern falling on the mask is identical to the pattern falling on the CCD camera (Fig. 4).
(3) The response of the bucket detector BD is the value of the total intensity that passes through the mask. According to the conventional procedure used in ghost imaging, the BD's response is the statistical weight of each pattern in the final average.

The first condition tells us that we should not treat all images reaching the CCD camera on an equal footing. Certain images are to be weighted more than others. Although the choice of a particular selection criterion is essential in ghost imaging, it is evident that, according to conditions (2) and (3), a selection criterion should be based only on the response of the bucket detector, because this response is the only parameter possessing a memory of the presence of a mask. An important issue is that there is not a universal rule for attributing a statistical weight to the useful images. Recall, for example, that a binary selection method was employed in Sec. II: the needlelike beam falling on the camera was either recorded or discarded. As we will see, more flexible rules can be adopted when the beam sections contain a random structure, as in ghost imaging with thermal light.

A. Ghost imaging with thermal light: Intermediate-size speckle

We describe here how we can reconstruct the image of a mask when the average size of the speckles produced by the twin beams is comparable to the dimensions of the apertures. A similar problem involving a double slit was solved theoretically and demonstrated experimentally in Ref. 14.

To assess the efficiency of speckle imaging it is essential to understand why the relative size of the speckle granularity affects the results. To this end we use a mask pierced by

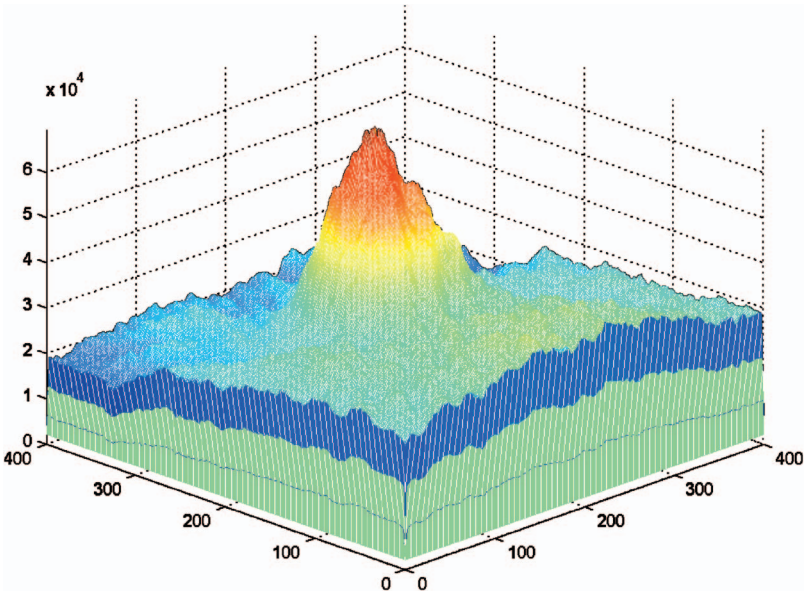

Fig. 5. Reconstruction of the object for a single hole mask; the threshold is kept at a low level. In Figs. 5–7 the average speckle size is about 300 μm.

three 1 mm holes, each of which can be closed if desired. The speckle size is about one-third of the hole dimensions and is significantly smaller than the hole-to-hole separation (4 mm). For completeness, we recorded the images that formed when one, two, or three holes were open.

According to point (3) of Sec. III, the image of the mask is recovered by summing the speckle patterns falling on the CCD camera (none of which interacts with the mask before being summed). Each CCD speckle pattern is multiplied by the output of the bucket detector produced in the other arm by the twin pattern impinging on the mask. We again emphasize that the value of this multiplier is unrelated to the shape of the mask and acts as a statistical weight assigned to each image in the final sum. The mathematics of this procedure given in Eq. (C5) is that a faithful image of the mask is obtained by the convolution of the mask transparency function with the autocorrelation function of the speckle pattern. This procedure has been successfully employed to compare theory to experiments on ghost imaging produced by thermal light.[9] In these experiments[10] the gate circuit G was not present, and the statistical weight assigned to each speckle pattern impinging on the CCD camera was provided by the value of the bucket output.

Before discussing some practical consequences of Eq. (C5), we ask if we can find a better method for improving the visibility of the reconstructed image; that is, a method more efficient than that of merely multiplying each speckle pattern by the value of the corresponding bucket detector output. We found that the efficiency can be improved; the explanation is simplest for the one-hole mask.

Suppose that the gate threshold has been set at a value below which a speckle pattern is rejected. In other words, a CCD pattern is admitted to the final summation only when the corresponding bucket detector output is sufficiently large, that is, when the mask aperture is sufficiently illuminated. In the one-hole case, each time the speckle pattern B1 is recorded by the camera, its twin pattern B2 must exhibit a bright speckle at the hole's position; otherwise, the bucket detector would not be able to send a gate pulse. Thus, the main effect produced by a proper setting of the threshold is that the speckle patterns summed by the CCD camera (and contributing to the final image) must all contain a bright spot at the hole's position. The consequence of this selection is that an enhanced image of the hole will emerge above the surrounding background noise (see Fig. 5). By proper setting we mean that the threshold level should be neither too low (no selection would be made) nor too high (only very few patterns would be summed and the statistical accuracy of the reconstructed image would be poor).

An analogous effect occurs for a two-hole mask, which can be described similarly. By setting the intensity threshold at some higher value, the gate statistically forces the CCD to record the speckle image only when there are two bright spots falling simultaneously on the two holes. It is clear that for a multi-hole mask the simultaneous occurrence of a bright spot at all holes (which is the desirable condition for maximum image visibility) becomes a less and less likely event as the number of holes increases with a consequent decrease of the visibility.[14]

The present paper demonstrates experimentally the image enhancement effect produced by the threshold selection we have described in the case of a two-hole mask (see Fig. 6, in which the visibility has been enhanced by setting the threshold at a level higher than in Fig. 5) and with a three-hole mask (see Fig. 7, which shows the different visibilities found by setting the threshold at two different levels).

We conclude this section by mentioning that as the speckles become larger than the holes, we first obtain a progressive blurring of the image, while in the large speckle limit (high spatial coherence) a conventional interference pattern will emerge due to the large spatial coherence of the beams.

B. Ghost imaging with thermal light: Small-size speckle

The small speckle condition (speckle size much smaller than the hole dimensions) is even more interesting from the statistical point of view. If we extrapolate the results of Sec. III A to the small speckle domain, we would initially be skeptical about the possibility of implementing an efficient

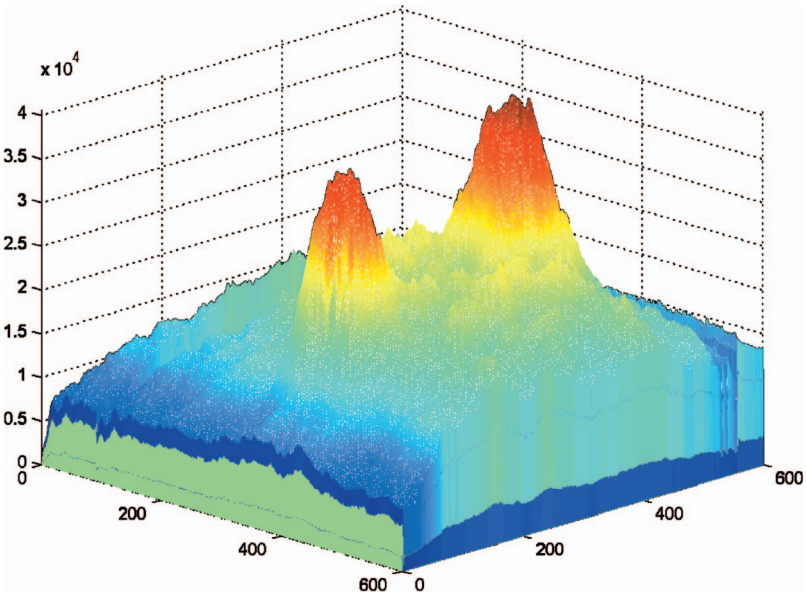

Fig. 6. Reconstruction of the object for a double hole mask; note the good visibility produced by a threshold level that is significantly higher than in Fig. 5.

thermal light imaging. The reason is that the number of speckles falling on each hole becomes large as the speckle size becomes small, and hence the relative fluctuations of the total intensity falling on the bucket detector might be naively expected to become smaller and smaller. Consequently, all images reaching the CCD camera would be given approximately the same statistical weight and, according to condition (1) of Sec. III, would produce a result essentially dominated by noise. This prediction seems to be confirmed by the fact[14] that the difficulty of obtaining acceptable images when the mask is complex increases when the speckles are small. This difficulty would be always present in practical cases, because a sensible imaging technique cannot be limited to holes of equal size. A complex mask is by definition inhomogeneous in the sense that a speckle of a given size will be large with respect to some details and small with respect to other details of the same image.

To understand how image retrieval is also possible in this case, we refer to the comment following Eq. (C5) that the mask function can be retrieved after removing (either by software or by an electronic circuit[15]) the usually large noise offset predicted by Eq. (C5). The reason for this conclusion

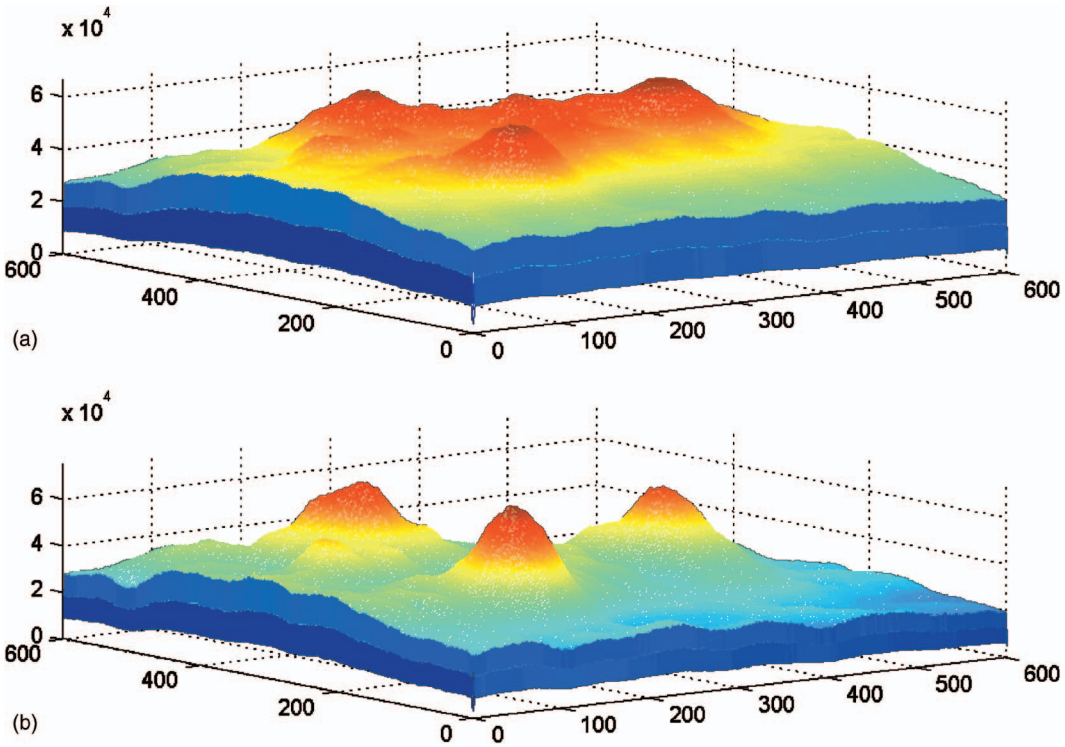

Fig. 7. Reconstruction of the object for a triple hole mask: (a) low threshold level and (b) high threshold level.

lies in the peculiar statistics of thermal light speckles, whose intensity follows a negative exponential distribution and accounts for the successful use of a threshold.

IV. GHOST IMAGING USING ENTANGLED PHOTON PAIRS

The first experiments on ghost imaging were performed using a pair of entangled photons produced by spontaneous parametric down conversion. In this process, a primary (pump) photon is incident on a nonlinear crystal and produces a pair of photons (idler and signal). These photons are correlated in energy, momentum, time of birth, and polarization.[1] Some of these features are exploited to match the needs of diverse experiments. Momentum conservation ($\mathbf{k}_{\text{pump}}=\mathbf{k}_{\text{idler}}+\mathbf{k}_{\text{signal}}$) in the "degenerate" case (when the idler and the signal photons acquire the same frequency) leads to the production of a pair of simultaneous photons that are emitted at equal angles relative to the incident beam.

As happens with quantum entangled states, the exact output direction of each individual photon cannot be predicted. But if we measure the output direction of one of them, we automatically acquire complete knowledge of the other photon's direction. This angular correlation allowed the realization of an EPR experiment and marked the official birth of ghost imaging.[1] Thus there is a beautiful and instructive link between ghost imaging produced by entangled photon pairs and the needlelike experiment discussed in Ref. 6. In the latter the angular correlations are generated by the mirror oscillations (plus a beam splitter behind it) rather than by spontaneous parametric down conversion. We could push the analogy even further by randomly chopping the needlelike beam to obtain correlated pairs of extremely short and simultaneous pulses.

The treatment of intensity ghost imaging produced by entangled photon pairs is not conceptually (and mathematically) different from the needlelike case, so that a specific discussion would be superfluous. The obvious experimental requirement is that the apparatus must be fast enough to detect the true coincidences in the arrival times of the entangled photons to avoid spurious coincidences that would spoil the results.

APPENDIX A: A SUMMARY OF LASER SPECKLES

The relevant properties of speckle patterns generated when coherent light is scattered by a rough surface (see Fig. 4) can be explained by the well known procedure used to derive the error function in elementary measurement theory. In this perspective it is instructive to interpret the Gaussian distribution as a function that describes the results of repeated one-dimensional random walks. A one-dimensional random walk is the sum of n steps along a line with the displacement at each step generated at random from a given probability distribution. In a two-dimensional random walk the steps are vectors in a plane rather than segments on a line. The central limit theorem implies that if the random errors are mutually independent and their number is large, the deviations from the mean are distributed according to a zero-mean Gaussian function.

Consider a population of n scatterers, randomly positioned in the path of a laser beam. The most common situation consists of a ground glass disk hit by a laser beam.[11] The jth scatterer becomes the source of an electromagnetic coherent wave that propagates to a far away screen, where it interferes with the waves generated by the other $(n-1)$ scatterers. The collection of bright and dark patches on the screen, resulting from the multiple interference of randomly dephased waves, is a speckle pattern. This qualitative description can be quantified by recalling that the electric field is a vector with a modulus and a phase. If we suppress high frequency oscillations (that is, terms like $e^{2\pi i\nu t}$, where ν is the laser frequency), we can describe the electric field as a complex number, often called a phasor. At a point P on the image screen, the electric field E will be given by the sum of the fields produced by the n scatterers:

$$E=\sum_{j=1}^{j=n} E_j e^{i\phi_j}, \tag{A1}$$

where ϕ_j is the phase acquired by the electromagnetic wave along the path joining the jth scatterer to point P, and E_j is the amplitude of the jth scatterer at P. Equation (A1) shows that the field at P is the sum of n phasors in the complex plane. It is easy to calculate the average values of the real and the imaginary parts of the electric field at P, from which the statistical distribution of the speckle intensity can be obtained. This demonstration is only outlined here because it is given in many textbooks.[12]

We begin by splitting Eq. (A1) into equations for the real and the imaginary parts. The real part gives

$$E^{(r)}=\sum_{j=1}^{j=n} E_j \cos(\phi_j). \tag{A2}$$

Thus $E^{(r)}$ is a one-dimensional random walk in which each step is the product of two random terms. Because of the smallness of the laser wavelength, the ϕ_j (modulus 2π) are usually uniformly distributed in the interval $(0,2\pi)$. Equation (A2) shows that if the random amplitudes and the random phases are independent, each term is a zero-mean random variable. We conclude that if the number of scatterers is large, the real part of E is distributed according to a zero-mean Gaussian function. A similar demonstration would show that the imaginary part of E is distributed in the same way. At this point, variable transformations commonly used in statistics show that the sum of the squares of $E^{(r)}$ and $E^{(i)}$, that is, the speckle intensity, follows a negative exponential distribution. This result is relevant to our work, because the long tail of the negative exponential distribution predicts that very high intensities are not exceptional, and consequently help to retrieve a well contrasted ghost image.

The average speckle dimension. Consider a point P at the center of a bright speckle. Around this point the n waves predominantly interfere constructively and generate a large field. How far can we shift from P without leaving this bright zone? As we move away from P, the distances to the n scatterers will change, increasing or decreasing by different amounts. To answer this question we may require that the typical path change be of the order of a wavelength. Elementary geometrical reasoning shows that the maximum allowed displacement from P (the size of the speckle) is of the order of λ/Θ, where Θ is the angular extension of the scattering region as viewed from P. This relation, which is confirmed in Appendix B, is essential for controlling the speckle size and is consistent with our setup parameters.

The spatial autocorrelation of intensity. If we make a plot of the light intensity on the image plane, we obtain a ridged

surface containing hills (bright speckles) and valleys (dark speckles). Because the cause of these corrugations is the interference of many waves coming from randomly located radiators, we cannot expect any regularity in the positions of the hills. This impossibility suggests that the only relevant spatial correlation is between a hill and itself. Thus if we define a correlation function by evaluating the average of the product $I(x)I(x+\Delta)$ as a function of Δ, we will obtain a hill centered around $\Delta=0$, which decreases to a noisy constant. It is also obvious that the horizontal extension of the central hill is the average size of the speckle grains. It is for this reason that when the speckles become very small, the spatial autocorrelation of the intensity reduces to a pronounced and narrow peak around $\Delta=0$. In ghost imaging this result is important for obtaining well defined images (see Sec. III B).

The temporal coherence of fluctuating speckle patterns. Suppose that the ground glass disk we have mentioned is initially nonrotating and thus the speckle pattern in the image plane is still. We now set the disk in motion. Some of the scatterers will begin exiting the laser spot and will be replaced by other scatterers that were initially outside it. This change alters the values of some of the random phases. When most of the original scatterers have been replaced by new ones, the new speckle pattern will be completely unrelated to the initial pattern. As the speckle pattern evolves, the light intensity at a given point P fluctuates with a characteristic time that is the time required for a relevant fraction of the scatterers to move out of the laser spot. This time is the coherence time τ_c of the process, a measure of the temporal extent over which we can predict the future values of the light intensity at a given point.

APPENDIX B: DESCRIPTION OF THE APPARATUS

It is convenient to fix the values of the optical parameters starting from the spatial resolution of the camera. The spatial resolution will be good if the mask apertures (in our case, the hole diameters) are larger than the pixel size. To obtain a final image of good visibility, a speckle size should be used that is about three times smaller than the width of the mask aperture. It is easy to satisfy the latter condition because the speckle size is related to the diameter of the laser beam impinging on the ground glass disk and to the distance of the mask from the disk;[11] both parameters can be varied within wide ranges.

In our experiment the choices of about 0.3 mm for the speckle size and 1 mm for the hole diameter were a consequence of the low spatial resolution of the only camera available to us at that time (18 lines/mm). The camera is a Proxitronic BV2561 intensifier optically coupled to a Thomson TH79KA96A. The light intensity generated by a 5 mW laser lets us use any common inexpensive camera with identical results. In a typical student laboratory the camera with a PC interfaced digitizing board is the most expensive component. The bucket detector BD is a common photodiode with an active area larger than the whole object mask OM.

After adjusting the speckle size to obtain good visibility, we required the distances d_A, d_B, and d'_B to satisfy

$$\frac{1}{d_B - d_A} + \frac{1}{d'_B} = \frac{1}{F}, \tag{B1}$$

where F is the focal length of the lens in Fig. 3. The electronic circuit allows the detector to gate the image intensifier

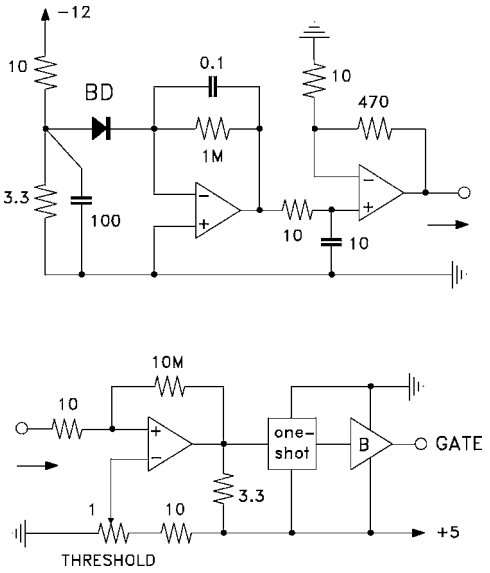

Fig. 8. Schematics of the experiment. The photodiode (BD) is the Hamamatsu S1226-8BK, but any device with an active area wide enough to cover the whole mask will work. Comparator: $\frac{1}{4}$LM339; one-shot: SN74121; line buffer (B): TC4422. Unless otherwise stated, resistor values are in kΩ and capacitor values in nF.

(see Fig. 8). We used a reversed biased Hamamatsu S1226-8BK photodiode, whose output is current-to-voltage converted, so that any FET operational amplifier, for example, the Texas TL081, will work. The output of this first amplifier is further amplified to obtain a root mean squared voltage level ranging from 100 to 400 mV at the noninverting input of an LM339 voltage comparator, while the other input of the comparator is kept at the voltage level set by the threshold control. The width of the standard TTL pulse, which is output by the one-shot module, then buffered (B), and finally sent to the gate input of the camera (see Fig. 8), sets the value of the camera exposure time. The latter must be much shorter than the coherence time of the varying light intensity to grab a virtually still image of the speckle pattern.

The speckle patterns generated by light beams falling on separate areas of the rotating disk are mutually uncorrelated.[11] Hence, the coherence time of the quasi-thermal light depends only on the disk angular velocity for a fixed geometry. For a given value of this velocity, the time interval between two consecutive frames should be significantly longer than the coherence time. This condition ensures the mutual independence of all speckle patterns acquired and summed by the camera.[10] In our experiment, the coherence time of the quasi-thermal light was about 50 ms, and the exposure time and the average interval between consecutive frames were 10 ms and 1 s, respectively.

APPENDIX C: HOW THE FINAL IMAGE IS RELATED TO THE MASK SHAPE AND TO THE STATISTICS OF THE LIGHT INTENSITY

We give here a derivation for a one-dimensional double "slit" mask because it contains many essential aspects of ghost imaging. The extension of this result to two-dimensional (and more general) masks is straightforward. The derivation (which is not restricted to the case of quasi-

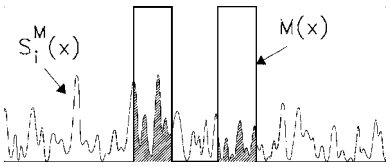

Fig. 9. $S_i^M(x)$ shows the profile of a typical intensity pattern falling on the mask; $M(x)$ is the mask transparency function. The shaded area represents the intensity passing through the mask; that is, the value measured by the bucket detector and is the weight w_i attributed to the same pattern $S_i^M(x)$.

thermal light) assumes the conventional ghost imaging retrieval based on the raw output of the bucket detector, without recourse to the threshold-based statistical weight discussed in Sec. III A.

Denote by $M(x)$ the transparency function of the mask, that is, $M(x)=1$ where the mask is transparent and $M(x)=0$ elsewhere. Now consider a sequence $\{S_i^M(x)\}$ $(i=1,\ldots,N)$ of N independent intensity patterns impinging on the mask. The superscript M stands for mask. The function $M(x)$ and a realization of the ith intensity pattern $S_i^M(x)$ are shown in Fig. 9. The random process responsible for the light intensity distribution is assumed to be stationary.

According to the procedure described in Sec. III A, we must evaluate the ith output, $w^{(i)}$, of the bucket detector; that is, the total intensity of the ith intensity pattern measured after the mask ($w^{(i)}$ is the statistical weight with which the ith intensity pattern contributes to the final image). In Fig. 9, $w^{(i)}$ is visualized by the shaded area. By changing the integration variable from x to y, $w^{(i)}$ can be expressed as

$$w^{(i)} = \int dy M(y) S_i^M(y). \tag{C1}$$

The final image $I(x)$ is the weighted average of the N patterns $S_i^C(x)$ falling on the camera (the superscript C stands for camera):

$$I(x) = \frac{1}{N}\sum_{i=1}^{i=N} w^{(i)} S_i^C(x). \tag{C2}$$

If we substitute Eq. (C1) into Eq. (C2), we obtain

$$I(x) = \frac{1}{N}\sum_{i=1}^{i=N} \int [dy M(y) S_i^M(y)] S_i^C(x)$$

$$= \int dy M(y) \langle S(y) S(x) \rangle, \tag{C3}$$

where the superscripts C and M have been suppressed because the light beams in the two arms are identical. We denote averages over the N patterns by angle brackets.

We now relate the term $\langle S(y)S(x)\rangle$ in Eq. (C3) to the centered autocorrelation function $C_S(x-y)$ of the stationary intensity pattern. The latter is defined as

$$C_S(x-y) = \frac{1}{N}\sum_{i=1}^{i=N} (S_i(y) - \langle S \rangle)(S_i(x) - \langle S \rangle)$$

$$= \langle S(y)S(x) \rangle - \langle S \rangle^2. \tag{C4}$$

By combining Eqs. (C3) and (C4) we obtain

$$I(x) = \int dy M(y) C_S(x-y) + \langle S \rangle^2 \int dy\, M(y). \tag{C5}$$

Some consequences of Eq. (C5) deserve comments, because they confirm some intuitive reasoning made in the text.

(1) The first term on the right-hand side of Eq. (C5) is the convolution of the mask function with the centered autocorrelation function of the intensity (which is a Gaussian for quasi-thermal light). The widths of the slits thus become larger and their borders smoothed.
(2) The second term on the right-hand side of Eq. (C5) is a pure noise offset, which lowers the image visibility. Scarcelli *et al.*[15] successfully removed it by means of a DC-block component inserted at the output of the light sensors.
(3) When the light is quasi-thermal and the average dimension of the speckles is very small with respect to the slit widths, the intensity autocorrelation function can be approximately written as $\delta(x-y)$. In this case Eq. (C5) yields $I(x)=M(x)+$ noise offset. This equation means that, in principle, a sharp reproduction of the mask function is possible after removing the noise offset. The smaller the speckle dimension, the larger the number of runs necessary to achieve a preset statistical accuracy.
(4) A beautiful conceptual link between the needlelike experiments considered in Sec. II and the thermal light experiments discussed in Sec. III can be given. In the former case, each beam's cross section is practically a point, that is, the function $S(x)$ is δ-like. From Eq. (C1) we see that in this case the statistical weight of the function $S_i^M(x)$ is 1 if the ray falls in the transparent part of the mask and is 0 elsewhere. This case is the binary selection rule for needlelike experiments described in Sec. II.

In summary, in quasi-thermal light experiments with very small speckles, the beams are endowed with a transverse intensity structure (speckles) whose spatial autocorrelation function is approximately a Dirac δ function. In needlelike beam experiments, the rays do not possess a transverse structure, but the Dirac δ function describes the intensity distribution of each ray. In both cases Eqs. (C1) and (C2) predict the possibility of recovering the mask function.

[a]Electronic mail: basano@fisica.unige.it

[1] D. V. Strekalov, A. V. Sergienko, D. N. Klyshko, and Y. H. Shih, "Observation of two-photon 'ghost' interference and diffraction," Phys. Rev. Lett. **74**, 3600–3603 (1995).
[2] D. N. Klyshko, "A simple method of preparing pure states of the optical-field, a realization of the Einstein, Podolsky, Rosen experiment and a demonstration of the complementary principle," Usp. Fiz. Nauk **154**, 133–152 (1988).
[3] D. N. Klyshko, *Photons and Nonlinear Optics* (Gordon and Breach, New York, 1989).
[4] T. B. Pittman, Y. H. Shih, D. V. Strekalov, and A. V. Sergienko, "Optical imaging by means of two-photon quantum entanglement," Phys. Rev. A **52**, R3429–R3432 (1995).
[5] A. F. Abouraddy, B. E. A. Saleh, A. V. Sergienko, and M. C. Teich, "Role of entanglement in two-photon imaging," Phys. Rev. Lett. **87**, 123602-1–4 (2001).
[6] R. S. Bennink, S. J. Bentley, and R. W. Boyd, "Two-photon coincidence imaging with a classical source," Phys. Rev. Lett. **89**, 113601-1–4 (2002).
[7] R. S. Bennink, S. J. Bentley and R. W. Boyd, "Quantum and classical coincidence imaging," Phys. Rev. Lett. **92**, 033601-1–4 (2004).
[8] A. Gatti, E. Brambilla, and L. A. Lugiato, "Entangled imaging and wave-

particle duality: from the microscopic to the macroscopic realm," Phys. Rev. Lett. **90**, 133603-1–4 (2003).
[9] A. Gatti, E. Brambilla, M. Bache, and L. A. Lugiato, "Correlated imaging, quantum and classical," Phys. Rev. A **70**, 013802-1–10 (2004).
[10] F. Ferri, D. Magatti, A. Gatti, M. Bache, E. Brambilla, and L. A. Lugiato, "High-resolution ghost image and ghost diffraction experiments with thermal light," Phys. Rev. Lett. **94**, 183602-1–4 (2005).
[11] W. Martienssen and E. Spiller, "Coherence and fluctuations in light beams," Am. J. Phys. **32**, 919–926 (1964).
[12] See for example, J. W. Goodman, *Statistical Optics* (Wiley, New York, 1985), pp. 44–50.
[13] P. W. Milonni and J. H. Eberly, *Lasers* (Wiley, New York, 1988), p. 577.
[14] A. Valencia, G. Scarcelli, M. D'Angelo, and Y. Shih, "Two-photon imaging with thermal light," Phys. Rev. Lett. **94**, 063601-1–4 (2005).
[15] G. Scarcelli, V. Berardi, and Y. Shih, "Phase-conjugate mirror via two-photon thermal light imaging," Appl. Phys. Lett. **88**, 061106-1–3 (2006).